INTERNATIONAL JOURNAL OF CLIMATOLOGY
Int. J. Climatol. **27**: 749–760 (2007)
Published online 1 November 2006 in Wiley InterScience
(www.interscience.wiley.com) DOI: 10.1002/joc.1435

RMetS
ROYAL METEOROLOGICAL SOCIETY

Understanding rainfall spatial variability in southeast USA at different timescales

G. A. Baigorria,[a,*] J. W. Jones[a] and J. J. O'Brien[b]
[a] *Agricultural and Biological Engineering Department, University of Florida, Gainesville, FL 32611-0570, USA*
[b] *Center for Ocean-Atmospheric Prediction Studies. The Florida State University. Tallahassee, FL 32312, USA*

Abstract:

This study seeks to understand the spatial variability of monthly and daily rainfall in Alabama, Georgia, and Florida, USA. Monthly spatial statistics are needed to improve downscaling from climate models producing seasonal rainfall forecasts, and spatial correlation of daily rainfall is needed to inform spatial weather generators used in climate risk analysis. We first determined the historical record length that is stationary followed by an analysis of the monthly spatial characteristics of rainfall variables. Rainfall data from 523 weather stations (National Climate Data Center) were obtained for the period 1915–2004 and divided into 15-year subsets for comparisons. Differences in rainfall were found between the most recent 15-year period and all others occurring during the 90-year period of record. Thus only data from 1990 to 2004 (208 weather stations) were used to avoid the detected changes in climate in the region. Correlation, covariance and variance matrices of daily and monthly rainfall amounts were calculated at monthly steps. The same statistics were also computed for frequency of rainfall events and monthly number of rainy days. Results show different spatial patterns at different temporal scales; two spatial patterns were well established. A widely spread correlation in a northeast – southwest direction was found around weather stations during the frontal rainy season, and a concentric short distance-decay in correlations existed around weather stations during the summer convective season. Spatial correlations among daily rainfall amounts are needed for spatial weather generators in a storm-by-storm basis while monthly spatial statistics are needed to ensure the validity of downscaled data from numerical seasonal rainfall forecasts. Copyright © 2006 Royal Meteorological Society

KEY WORDS rainfall; climate; spatial variation; correlation matrix; semivariograms

Received 8 June 2006; Revised 30 August 2006; Accepted 2 September 2006

INTRODUCTION

Rainfall varies considerably over space and time. Agricultural systems have evolved in response to this variability, but in most regions of the world, rainfall variability continues to be a major source of risks that farmers face. Depending on spatial extent and persistence of drought, for example, entire communities and regions risk economic and food security problems. Research is being conducted to better understand climate variability, its impacts on agricultural systems, and how to reduce those risks through decisions and policies that consider climate variability.

Crop models (Jones *et al*., 2003) are now widely used to analyze climate variability impacts on agricultural systems. The availability of daily weather variables over long time periods continues to be a problem in most regions of the world. Variability is so high that only a few years' data cannot capture its magnitude. In order to have sufficient lengths of record, statistical methods are used to generate daily realizations of rainfall and other variables for use in crop models for many applications (Podestá *et al*., 2002; Hansen and Indeje, 2004; Baigorria, 2005). These daily stochastic weather generators are also used to downscale climate forecasts for use in models (Briggs and Wilks, 1996; Grondona *et al*., 2000; Wilks, 2002). One goal of our research is to use daily weather generators to downscale 6-month climate forecasts from The Florida State University global/regional climate model (Cocke and LaRow, 2000) coupled with the Community Land Model (Bonan *et al*., 2002; Zeng *et al*., 2002) – FSUCLM (Shin *et al*., 2005) to any point in SE-USA.

The problem with most currently available weather generators (Richardson and Wright, 1984; Racsko *et al*., 1991; Parlange and Katz, 2000; Schoof *et al*., 2005) is that they create daily realizations for points in space without considering spatial correlation or persistence of rainfall events and amounts over space (Clark *et al*., 2004; Fowler *et al*., 2005). This is not a problem if one's interest is in statistical properties of rainfall, other weather variables, and crop production at points or fields. But if spatially independently generated weather data are used to aggregate rainfall or crop model outputs over space, for subsequent analyses of these aggregated variables, spatial

* Correspondence to: G. A. Baigorria, Agricultural and Biological Engineering Department, University of Florida, Gainesville, FL 32611-0570, USA. E-mail: gbaigorr@ifas.ufl.edu

correlations of the variables must be taken into account for the same timescale at which the data are used as inputs to models. Because crop models respond to rainfall on a daily basis, even if 2 months have the same rainfall but different temporal distributions during the month, simulated results may differ widely. One example is analyzing statewide production variability over time (years) where state production is aggregated over model simulations at many locations with significant correlations in daily rainfall among locations. In hydrological modeling, the spatial distribution of precipitation may have considerable effects on the discharge of a river and the occurrence of floods or droughts (Baigorria and Romero, 2006).

A number of questions arose as we were considering how to incorporate spatial correlations in generating rainfall over large areas. For example, what are the inherent correlations of rainfall across the SE-USA, and how do those correlations vary with time? Are correlations of rainfall over space the same for monthly and daily rainfall amounts? This study was conducted to help answer these questions and to guide us in designing a daily weather generator that will produce realizations of daily weather that preserves spatial patterns of the original data. Objectives were: (1) to quantify spatial correlations of daily rainfall events and daily amounts over this region, (2) to determine how these correlations vary during the year, and (3) to compare spatial correlations at daily and monthly timescales.

STUDY AREA

The study area includes the states of Alabama, Florida and Georgia in the SE-USA between 35°23′ N, 88°59′ W and 24°57′ N, 79°26′ W. The area ranges between 0 and 1435 meters above sea level and covers a total area of 421 072 km^2. These three states constitute the working area of the Southeast Climate Consortium – SECC (http://www.agclimate.org; Vedwan *et al*., 2005). This is a group of six universities in the SE-USA working in research and extension of the effects of climate variability and risk management in agriculture, forestry and water resources.

This region has some of the warmest conditions in the United States. However, it is the only region in the United States to show widespread but discontinuous cooling periods of 1–2 °C over almost the entire area during the past 100 years (Karl *et al*., 1993; Fraisse *et al*., 2006). The annual rainfall ranges from 1100 mm to 1400 mm, with the highest annual precipitation occurring along the Gulf of Mexico coast and in south Florida (USGS, 2006). Rainfall occurs throughout the year caused by two different processes. During most of fall and winter, rainfall occurs mainly by fronts coming from the northwestern United States crossing the area (Frontal rainy season; FR). During most of spring and summer, rainfall occurs mainly by convective processes and tropical storms (convective rainy season; CR). The temporal trend in annual precipitation shows that rainfall has increased

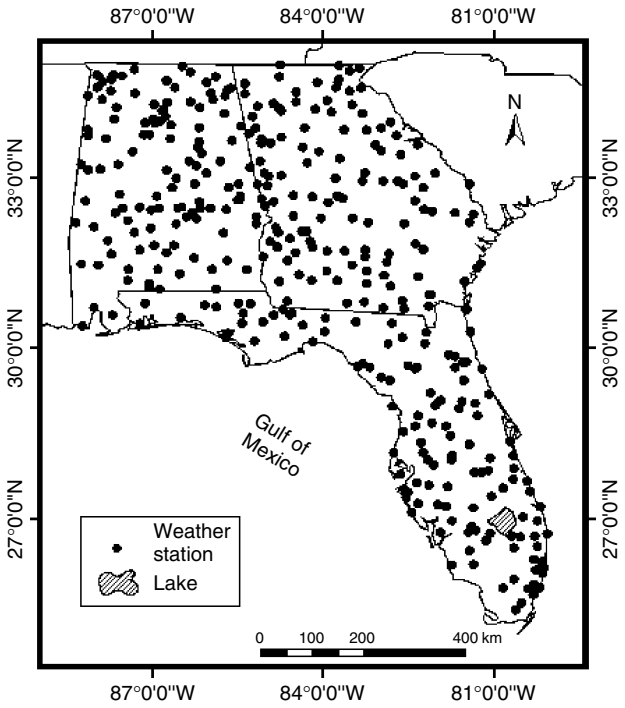

Figure 1. Weather station network.

by 20–30% or more over the past 100 years across Mississippi, Arkansas, South Carolina, Tennessee, Alabama, and parts of Louisiana, with mixed changes across most of the remaining area (SRAT, 2002).

Trends in wet and dry spells during the twentieth century, as indicated by the Palmer drought severity index (PDSI), are spatially consistent with the region's annual precipitation trends, showing a strong tendency to more wet spells in the Gulf Coast states, and a moderate drought tendency in most other areas. The percentage of the southeastern landscape experiencing severe wetness (periods in which the PDSI averages more than +3) increased approximately by 10% between 1910 and 1997 (Soule, 1993; SRAT, 2002).

DATA AND METHODOLOGY

Weather station network

The historical daily weather data record from 1048 weather stations was obtained from the National Climate Data Center (http://nndc.noaa.gov/?home.shtml). The period from 1915 to 2004 was selected from this record due to the quality and quantity of the rainfall data. This information was organized and checked for errors and missing values. Range errors and zeros substituted for replacing missing values were identified and deleted. For monthly analyses, months with fewer than 20 days for which data were recorded were not considered. Weather stations beyond their state and county limits for which coordinates could not be corrected were deleted. After this screening process, 523 weather stations remained for further analyses; Figure 1 shows the spatial distribution of the weather stations.

DOI: 10.1002/joc

Figure 2(a) shows a histogram summarizing the number of weather stations and their lengths of record. Fewer than 25 weather stations had the 90-year historical record almost complete. Figure 2(b) shows the temporal variability of the network. This variability reflects the changing support for collecting this kind of information by governmental agencies.

Selecting the historical record length for spatial analyses

Before analyzing the spatial correlations of daily and monthly rainfall data, we analyzed the data to determine whether significant shifts in rainfall had occurred over the 90 years of record. Few weather stations had a complete 90-year historical record, making it difficult to identify these shifts. Therefore all available monthly weather station data across the 90-year period were spatially interpolated using ordinary Kriging. This interpolation method estimates data as weighted linear combinations of the available data, trying to have the mean residual equal to zero, and minimizing the variance of the error (Isaaks and Srivastava, 1989). The interpolation was performed in the residuals after removing the spatial trends. In doing so, we avoid the need to interpolate the geographical trend due to not fulfilling the stationary assumption of semi-variogram models (Clark and Harper, 2001; Goovaerts, 1997). Observed data at weather stations were preserved during these interpolations. Resulting monthly maps were divided into 6 periods of 15 years each and statistically compared using analysis of variance F statistic followed by a Duncan's multiple range test for each grid cell.

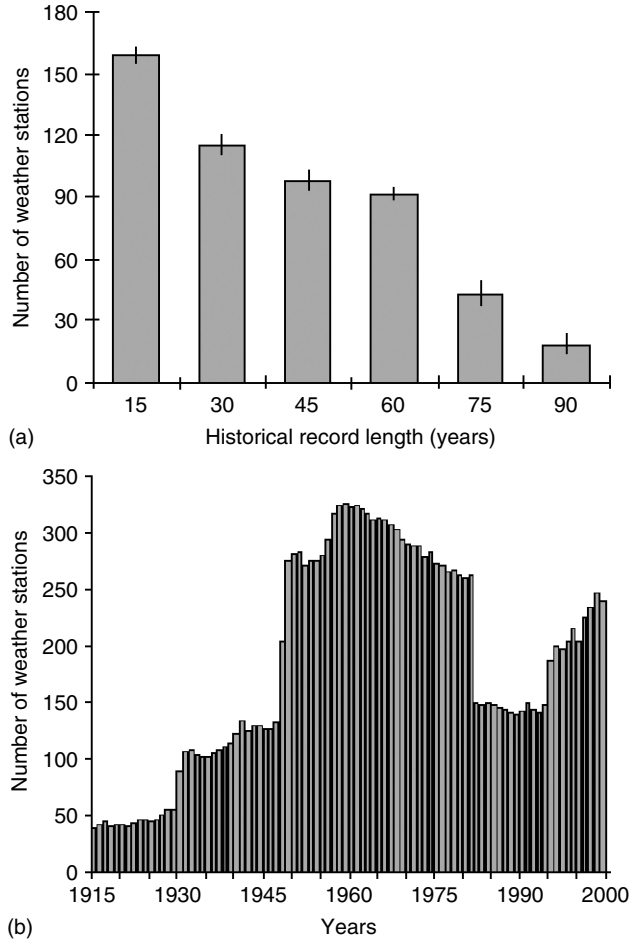

Figure 2. Temporal analysis of the weather station network.

De-trending the spatial data. Most geo-statistical techniques assume that sample data come from a fixed distribution. Because there were spatial trends in the rainfall values, the trends were modeled by a polynomial equation using latitude and longitude as predictors (Clark and Harper, 2001). Polynomial equations from first to third degree were fitted by using least squares method. The degree of the polynomial equation for each month and year was selected by comparing the sum of the squared residuals as a percentage of the original variation. This process yielded 1080 polynomial equations of first and third degrees. Afterwards, trend values were calculated and subtracted from the monthly-observed rainfall values to compute residuals. These residuals were not significantly different from a normal distribution for all cases. Then, for each month and year, semivariograms were calculated using the following algorithm (Isaaks and Srivastava, 1989; Table I):

$$\gamma(h) = \frac{1}{2N(h)} \sum_{(i,j)|h_{ij}\approx h} (x_i - x_j)^2 \qquad (1)$$

Table I. Variable description.

Symbol	Definition	Units
i, j	Weather stations	Unitless
x_i, x_j	Rainfall amount at weather stations i and j	mm
μ_i, μ_j	Mean rainfall amount at weather stations i and j	mm
σ_i, σ_j	Standard deviation rainfall amount	mm
$\gamma(h)$	Semi-variance at distance h	mm^2
$\hat{\gamma}(h)$	Estimated semi-variance at distance h	mm^2
n	Number of observations	Unitless
$N(h)$	Number of pairs of weather stations whose location are separated by h	Unitless
h	Distance	Km
δ_0	Nugget (vertical jump from the value of 0 at the origin to the value of the semivariogram at small distances)	mm^2
δ_1	Sill (the semi-variance at which semivariogram reaches a plateau after adding δ_0)	mm^2
A	Range (the distance at which the semivariogram reaches a plateau)	Km
β	A parameter ranging from 0 to 2	Unitless
ρ_{ij}	Correlation between weather stations i and j	Unitless
C_{ij}	Covariance between weather stations i and j	mm^2
V_{ij}	Variance between weather stations i and j	mm^2

DOI: 10.1002/joc

After obtaining the $\gamma(h)$ values, models were fit to describe the changes in variance of rainfall amounts *versus* distance from each station, using a weighted nonlinear least-squares method (Jian *et al*., 1996; Whelan *et al*., 2001). The model used to fit the semivariograms was the Stable model (Whelan *et al*., 2001) defined as (Table I):

$$\hat{\gamma}(h) = \delta_0 + \delta_1 \left[1 - e^{-(h/A)^{\beta}}\right] \quad (2)$$

The Range (A), Nugget (δ_0) and Sill (δ_1) were then analyzed. To preserve the observed data where weather stations were located, the Nugget was always forced to 0. The sum of squared error (SSE), the root mean square error (RMSE) and Akaike information criterion (AIC; Webster and McBratney, 1989) were evaluated to determine the best-fit model. The AIC evaluates the goodness of fit as well as the parsimony of the model. Smaller values of AIC determine the best model.

After the semivariogram models were fit, monthly rainfall residuals were interpolated by using ordinary Kriging to obtain monthly maps of the residuals in a 5 km × 5 km grid resolution. The spatial trends were added to these interpolated residuals, yielding the monthly rainfall maps for all the 90 years of historical record. Interpolation errors related to the sample spatial variation are discussed in more detail in Section Analysis using Daily Data.

Statistical analysis of climate. These statistical analyses were performed to find areas where rainfall mean and variance were statistically different in time, i.e. areas affected by changes in climate. The 90-year historical record was divided into six periods of 15 years each (1915–1929, 1930–1944, 1945–1959, 1960–1974, 1975–1989 and 1990–2004). All analyses were performed monthwise.

The six 15-year periods were statistically compared through an analysis of variance F statistic (ANOVA F statistic) for each grid cell (5 km × 5 km cell size). The probability value (P-value) that the F test statistic is at least as large as the observed F value was assessed by using the F distribution table ($\alpha = 0.05$) with 5 and 84 degrees of freedom. After the P-values were calculated for each grid cell, they were spatially aggregated to obtain probability maps of statistical differences. Each map showed areas where statistically significant changes of monthly rainfall amounts were found in at least one of the six 15-year periods.

Because some areas showed statistically significant differences, the next step was to determine when these differences occurred. This was done in order to select the number of years to use to analyze spatial variability of current climate conditions for use in this study. Duncan's multiple range tests were performed for each grid cell across the domain. Results were spatially aggregated producing maps; however in this case, five maps for each month were generated. Each map compared the latest period of record (1990 through 2004) *versus* one of the five remaining 15-year periods.

Correlation, covariance and variance of rainfall over space

To avoid the effects of climatic shifts detected in time in the study area, only the period from 1990 to 2004 was used for further analysis. For this period, 208 weather stations were available. In this section, we determined how the correlation (ρ_{ij}), covariance (C_{ij}) and variance (V_{ij}) vary monthly during the year by using daily and monthly rainfall amounts and frequencies.

Analyses using daily data

Rainfall amount. Daily rainfall data from this 15-year period were split into 12 monthly subsets. Each subset, containing 15 years of daily rainfall data, was used to calculate ρ_{ij}, C_{ij} and V_{ij} among all the weather stations, thus forming matrices of rank 208. To avoid overestimation of ρ_{ij}, and C_{ij} as well as the underestimation of V_{ij}, days without rainfall at both weather stations were not used. The calculations were performed using the following equations (Table I):

$$\rho_{ij} = \frac{C_{ij}}{\sigma_i \sigma_j} \quad (3)$$

$$C_{ij} = \frac{1}{n} \sum (x_i - \mu_i)(x_j - \mu_j) \quad (4)$$

$$V_{ij} = \frac{1}{n} \sum (x_i - x_j)^2 \quad (5)$$

The distance, in kilometers, between each pair of weather stations was calculated by using its geographical coordinates and applying the Pythagorean theorem. Results from the three statistics at different distances were analyzed as monthly scatter plots. Because of the scatter in the data, results were classified into five distance classes: 0–50 km, 50–150 km, 150–350 km, 350–700 km and 700–1400 km. For each class, the means and the standard deviations of the three statistics were calculated.

To visualize the spatial variability of ρ_{ij} of one weather station (i) against the remaining (j), one weather station from each state was used as an example. The selected weather stations were: Sylacauga, Talladega, Alabama (33° 12′ N latitude, 86° 16′ W longitude, and 149 m altitude), Mountain Lake, Polk, Florida (28° 56′ N latitude, 81° 36′ W longitude, and 38 m altitude), and Hawkinsville, Pulaski, Georgia (32° 17′ N latitude, 83° 28′ S longitude, and 83 m altitude). Thus, values of ρ_{ij} were assigned at the geographical coordinates of the remaining 207 weather stations. At the selected weather stations (i), ρ_{ii} was assigned the value of 1.0. Finally, all the values were interpolated using ordinary Kriging. The analysis was performed taking only one of the three selected weather stations at a time. Results are presented for the months of January and July.

Occurrence of rainfall events. To calculate the ρ_{ij}, C_{ij} and V_{ij} matrices of occurrence of rainfall events, values of 1 and 0 replaced the values of rainfall amount for days with and without rainfall, respectively, over the 15-year

DOI: 10.1002/joc

period used in the study. As in the previous step, the data were divided into monthly subsets. Afterwards, Equations (3)–(5) were applied to each sub-dataset containing the 208 weather stations, thus producing the respective matrices. The data were further divided into the same five distance-based classes of the previous step for further analysis. To visualize the spatial correlation (ρ_{ij}) of one weather station *versus* the remaining stations, the same three weather stations selected in the previous step were used. Ordinary Kriging was used to interpolate the ρ_{ij} values.

Analyses using monthly data

Rainfall amount. Rainfall data aggregated at different temporal scales explain different spatial processes and relationships among weather stations. To understand the effects of this temporal aggregation, for each year and weather station, the total monthly rainfall amount was computed by summing all daily values in the month. Next, the 15-year period was divided into subsets for each of the 12 months of the year. Equations (3)–(5) were then modified for analyzing monthly rainfall values. These modified equations were applied to the monthly sub-datasets for obtaining the ρ_{ij}, C_{ij} and V_{ij} matrices. As before, results were classified according to their distances between stations. Finally mean and standard deviation of each distance-based class were calculated.

To visualize the spatial variability of ρ_{ij}, the same three weather stations selected in the previous step were used. Ordinary Kriging was used to interpolate the ρ_{ij} values.

Monthly number of rainy days. To perform this analysis, the number of rainy days was computed for each month of each year of the 15-year period. As in the previous step, the dataset was divided into subsets for the 12 months of the year. For each subset, Equations (3)–(5) were modified to compute ρ_{ij}, C_{ij} and V_{ij} for the number of rainy days per month. The same methodologies used in the steps before for estimating mean and standard deviation of ρ_{ij} in the distance-based classes as well as the correlation's spatial variability visualization were used for this variable.

RESULTS AND DISCUSSION

Changes in rainfall over the 90-year time period

The spatial trends of monthly rainfall amounts over 90 years from December to April followed first-degree polynomial equations. For the remaining months, the trends corresponded to a third degree polynomial equation. These monthly spatial trends were used for interpolation, and will also be used later to evaluate the spatial structure of seasonal rainfall forecasts and spatial weather generator performance. These polynomial equations explained from 40 to 81% of the rainfall spatial variability when aggregated over the 90-year period. Analyzing individual trends by month and by year (Table II), these percentages explained on average from 31 to 55% of the spatial variability. However, for individual months and years, these trends explained up to 91% of the spatial variability.

Figure 3 shows maps of probabilities (P-values) of monthly rainfall amounts that were significantly different for the different 15-year periods of time for January and July. Areas shown as dark brown indicate areas where at least one of the 15-year periods was significantly different from the others. White represents areas where there were no significant differences in rainfall amounts in any of the time periods. Areas where statistical differences were found varied monthly. This suggests that the processes leading to the changes were not due to local conditions but are more related to broader climatic processes.

After finding these significant differences, Duncan's Multiple Range Test was used to determine whether each 15-year period(s) of time differed from the latest period of record (1990 through 2004). Figure 4 shows the areas for January and July where significant differences occurred. January maps indicated that the Panhandle of Florida, southeastern Alabama and part of southwestern Georgia showed significantly different rainfall regimen in the last 15 years. July maps indicated that central western Georgia showed a significantly different rainfall regimen in the last 30 years when compared to earlier periods. For January, monthly rainfall in those changed areas increased over time while during July, monthly rainfall decreased. This is consistent with the report by Maul and Hanson (1990) and Stahle and Cleaveland (1992) and is possibly related to the less common summer blocking pattern of the Atlantic Subtropical Anticyclone reported by Davis *et al*. (1997).

These results demonstrated statistically significant spatial and temporal changes in the rainfall regimens during the last 90 years. Climate was not stationary in time, and as a consequence, a large number of years did not necessarily produce the lowest errors in forecasts based on climate normals (Huang *et al*., 1996). Our goal was to

Table II. Statistics of the monthly coefficients of determination (r^2) obtained from the year by year polynomial equation fitting.

Month	Mean	Standard deviation	Maximum	Minimum
January	0.408	0.228	0.823	0.002
February	0.380	0.231	0.798	0.011
March	0.378	0.236	0.837	0.000
April	0.313	0.199	0.794	0.001
May	0.396	0.173	0.823	0.068
June	0.434	0.182	0.832	0.099
July	0.387	0.159	0.780	0.099
August	0.431	0.149	0.874	0.114
September	0.506	0.166	0.832	0.153
October	0.532	0.189	0.908	0.133
November	0.545	0.180	0.836	0.070
December	0.403	0.219	0.807	0.014

DOI: 10.1002/joc

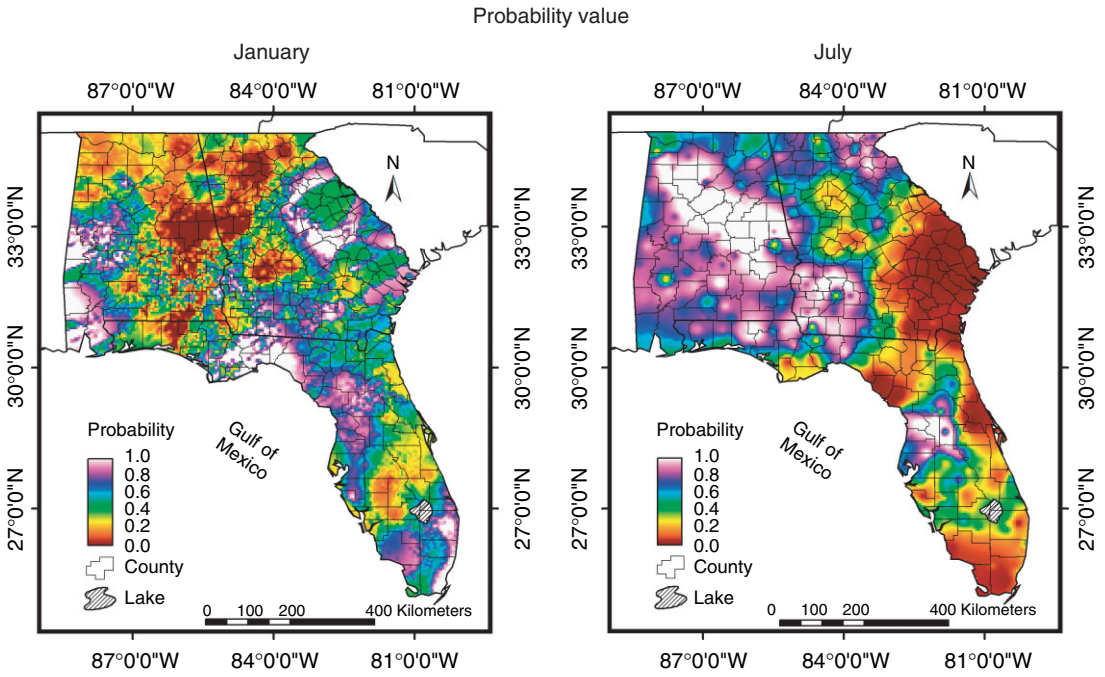

Figure 3. Maps of probability value where the f test statistics from ANOVA is at least as large as the observed f value ($\alpha = 0.05$). Comparison between the months of January and July.

provide information on spatial characteristics of current rainfall regimes for downscaling numerical climate forecasts and for generating spatially coherent rainfall events and amounts. Under this framework, the optimal time period to maximize the skill in predicting the upcoming year condition corresponded to the last 15-year period. Thus, further spatial analyses used only the 1990 through 2004 rainfall data.

CORRELATION, COVARIANCE AND VARIANCE

Analyses using daily data

Rainfall amount. Each point in Figure 5 represents the covariance of rainfall between each station and one other specific station, computed using the daily data for the 15 years for each month. Thus, there was a maximum of about 450 days of data to estimate each point, but this was reduced since only days when rainfall occurred in at least in one station were used. The shape of the cloud of points and the absolute values were similar during both Spring–Summer and Fall–Winter seasons, and similar between those seasons. However at short distances, March and September showed higher covariance values than the other months. These are the transitional months (around the solstices of winter and summer, respectively, for the northern hemisphere). These months are also the transition between the frontal rainy (FR) season from October to March, and the convective rainy (CR) season from April to September.

As expected, the correlation of rainfall amounts over space decayed *versus* distance, and the variance increased with distance (Sumner, 1983). Correlation indices at all distances were higher during the FR season than during the CR season (Table IIIa). Correlations during the CR season were statistically nonsignificant at closer distances than during the FR season. On the other hand, monthly standard deviations increased *versus* distance but did not show any apparent relationship to the FR and CR seasons. During the CR season, correlations did not exceed values of 0.8, while values near 1.0 did occur during the FR season. High variance values were found at short distances during the CR season in comparison to the FR season.

At short distances, there were also some low correlation and covariance values as well as high values of variance. Different rainfall regimens can be expected when daily data are analyzed (Romero and Baigorria, 2006). In the Peninsula of Florida, for example, weather stations located near the Atlantic coastline had a different rainfall regime than those near the Gulf of Mexico coastline. Similarly, weather stations near the coastline may differ from those further from the inland. Thus, rainfall is not stationary over space, which would violate assumptions used in computing semivariograms with only one realization of spatial data unless the data are de-trended.

Figures 6 and 7 showed spatial patterns in ρ_{ij} in all directions. Variations in the absolute values of ρ_{ij} showed higher correlations (lower variances) around the selected weather stations during the FR season (Figure 6) than during the CR season (Figure 7). This is explained by the size of the weather fronts or cells involved in the precipitation process. Areas with high correlations and low variances were larger during the FR season than during the CR season. Correlations were less concentric in January than in July. Both correlations and variances showed a more diagonal pattern during the FR season than during the CR season. There was more

DOI: 10.1002/joc

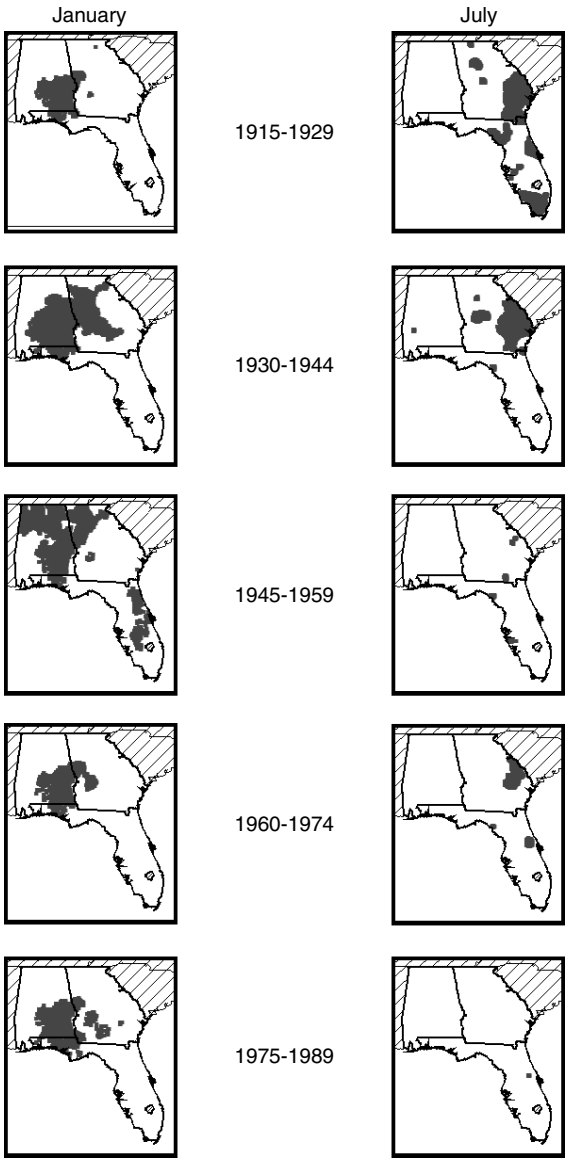

Figure 4. Maps of Duncan's multiple range tests ($\alpha = 0.05$) for the months of January and July.

directionality (anisotropy) (northeast–southwest) in the spatial variation of ρ_{ij} during the FR season than during the CR season. This directionality was parallel to the usual weather front patterns in this region as documented by Robinson and Henderson (1992) and Walsh *et al.* (1982). In the case of daily spatial variation of ρ_{ij} and in concordance with Sharon (1974), rainfall occurring from convective systems (CR season) typically showed correlations that decrease rapidly in all directions over short distances.

Occurrence of rainfall events. These results showed how each rainfall event was correlated with rainfall events at other weather stations on a daily basis. This variable responded similarly to that for ρ_{ij} values relative to the FR season *versus* the CR season (Table IVa). However, monthly variations in the maximum and minimum correlations for rainfall occurrences were less than those for daily rainfall amounts. Individual correlation values for July showed a maximum of 0.65 compared with the maximum in January of 0.9; however, both of these values were lower than those obtained for rainfall amount. The V_{ij} cloud shape in July (not shown) increased faster over short distances than in January, where low variance values were found at about 400 km or less. Despite variances during January and July reaching values greater than 0.4, in general terms, variance in January reached a plateau of around 0.23, while in July it reached a plateau around 0.30, both around 250 km from the station.

Spatial variations of daily rainfall event correlations showed similar characteristics as those for daily rainfall amount in terms of seasonal differences (Figures 6 and 7). Concentric and short distance decay functions occurred around selected weather stations for the CR season (Figure 7), while they were widely spread in a northeast–southwest direction for the FR season (Figure 6). For all weather stations, the FR season showed higher correlations than the CR season.

Analyses of monthly data

Rainfall amount. High correlations in monthly rainfall amounts were found as far away as 600 km from the selected stations during January (Figures 6 and 7). In July however, these same values occurred around 200 km or less. Larger numbers of negative correlations as well as higher variances were reached at shorter distances during July than during January, which corresponds to the different atmospheric physics producing the rainfall. Variances during the CR season had maximum values around 24 000 mm^2, while for the FR season values reached a maximum of only 16 000 mm^2.

There were differences in spatial patterns of rainfall amount correlation values relative to those found for daily rainfall data (Table IIIa) (*versus*) monthly rainfall data (Table IIIb). Positive correlation values higher than 0.8 were found using monthly rainfall amounts, while for daily data, all correlations were less than 0.7 (Tables IIIb (*versus*) 3a, respectively). Higher standard deviations of correlation values were found using monthly data compared to daily data. Correlation values and homogeneous correlation areas using monthly data were respectively higher and larger than the ones using daily data, independent of the analyzed month (Figures 6 and 7). This was because using daily data, rainfall amounts were correlated on a storm-by-storm basis. This, together with the rainfall event data, showed the size of the rainfall cell producing rainfall in a specific event. For using in a daily spatial weather generator, the highly correlated areas showed the size of the areas that would be involved in a storm event and how much rainfall would fall in every rain gauge. Spatial relationships among different monthly rainfall variables are governed by different climatic, oceanic, topographic and/or geographic drivers at different times. Thus, monthly spatial statistics would be useful to ensure the validity of downscaling data from numerical seasonal rainfall forecasts, which are produced based on atmospheric circulation patterns.

DOI: 10.1002/joc

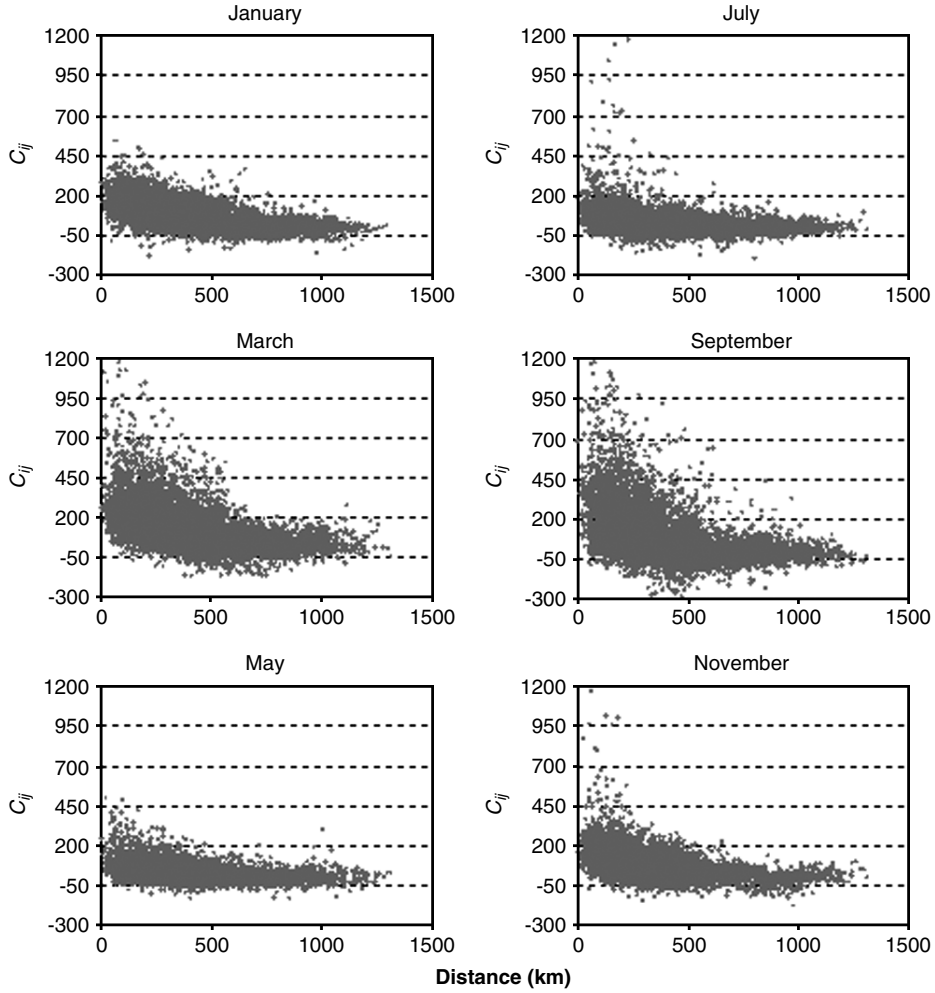

Figure 5. Monthly variation of the covariance matrices for daily rainfall amounts *versus* distance for six months of the year (1990–2004).

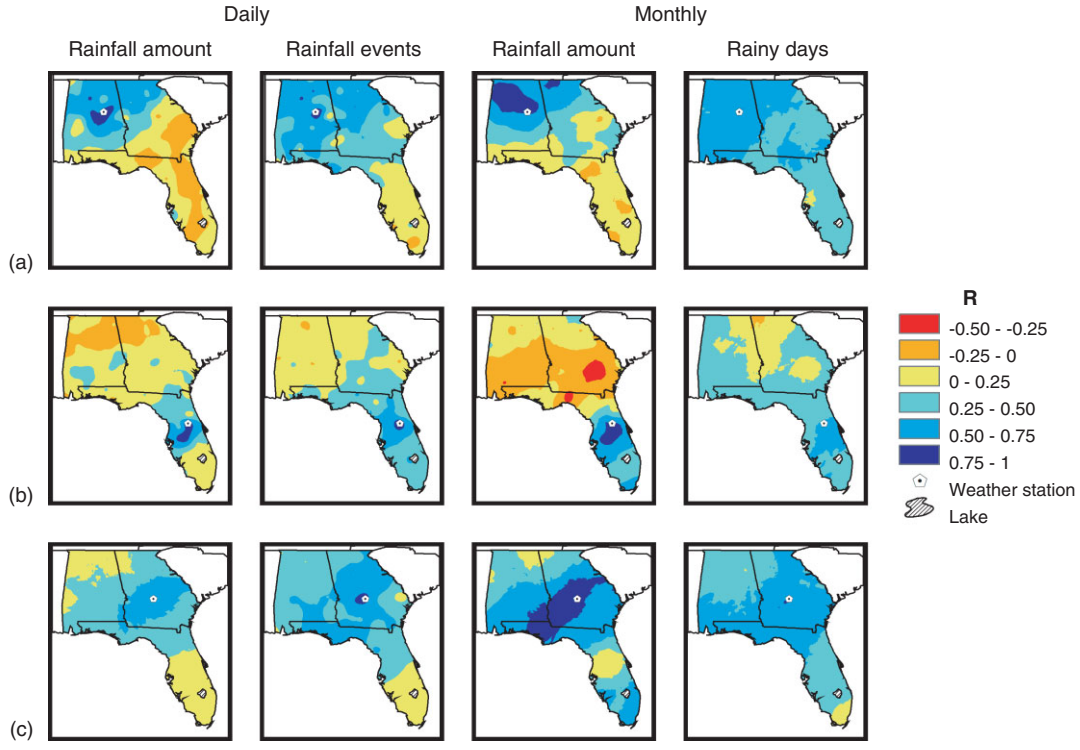

Figure 6. Correlation's spatial variability of daily rainfall amount, daily frequency of rainfall events, monthly rainfall amount and monthly number of rainy days for the month of January (1990–2004). (a) Sylacauga, (b) Mountain Lake and (c) Hawkinville.

DOI: 10.1002/joc

Monthly number of rainy days. The number of rainy days (days with measured rainfall larger >0.1 mm) divided by the total number of days was an estimate of the probability of rainfall in a specific month and weather station. Thus, the correlation among weather stations showed how rainfall occurrence was likely to persist over space. Table IVb showed that even though the absolute number of rainy days varied from season to season, there was no seasonal pattern in the correlation values. Figures 6 and 7 showed that homogeneous areas of correlation were larger compared with the daily occurrences of rainfall events. Correlation values were less concentric around the weather station using monthly data than daily data.

CONCLUSIONS

In the SE-USA, changes in rainfall amounts during the last 90 years were observed. These changes varied over space and time of the year. To avoid influences of climate change in our study, only the last 15-year period was used to characterize rainfall spatial variability. For this time

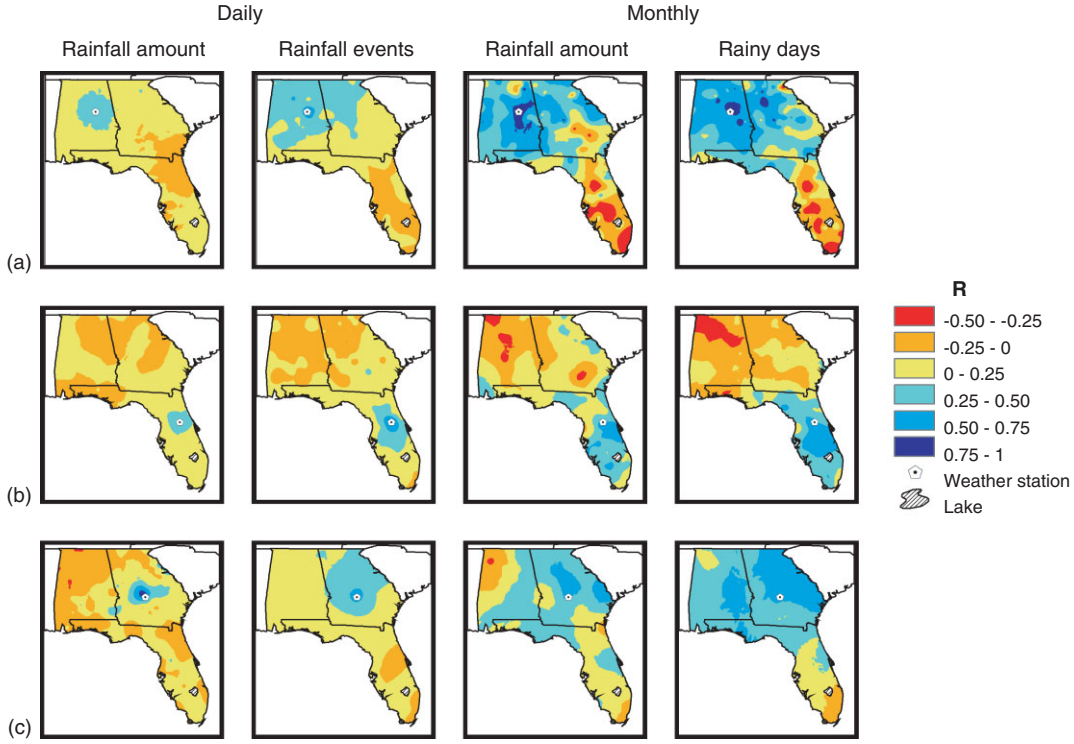

Figure 7. Correlation's spatial variability of daily rainfall amount, daily frequency of rainfall events, monthly rainfall amount and monthly number of rainy days for the month of July (1990–2004). (a) Sylacauga, (b) Mountain Lake and (c) Hawkinville.

Table III. Monthly correlation's statistics of (a) daily and (b) monthly rainfall amount, according to distance-based classes.

(a) Month	Distance (km)									
	0–50		50–150		150–350		350–700		700–1400	
	Mean	Standard deviation	Mean	Standard deviation	Mean	Standard deviation	Mean	Standard deviation	Mean	Standard deviation
January	0.663	0.185	0.527	0.208	0.348	0.208	0.138	0.182	0.036	0.132
February	0.648	0.152	0.493	0.202	0.311	0.207	0.157	0.158	0.104	0.162
March	0.671	0.184	0.534	0.197	0.381	0.191	0.193	0.183	0.104	0.164
April	0.594	0.180	0.427	0.203	0.278	0.181	0.129	0.162	0.039	0.170
May	0.473	0.174	0.270	0.210	0.157	0.189	0.057	0.175	0.009	0.166
June	0.383	0.157	0.194	0.159	0.097	0.148	0.039	0.134	0.013	0.136
July	0.368	0.177	0.191	0.199	0.088	0.162	0.024	0.133	0.005	0.124
August	0.376	0.195	0.163	0.172	0.066	0.161	0.014	0.140	−0.001	0.137
September	0.586	0.179	0.398	0.236	0.230	0.225	0.037	0.179	−0.036	0.138
October	0.651	0.163	0.495	0.228	0.345	0.226	0.182	0.214	0.006	0.163
November	0.616	0.187	0.445	0.220	0.279	0.207	0.126	0.167	0.027	0.165
December	0.662	0.148	0.520	0.203	0.322	0.209	0.144	0.199	0.012	0.162

DOI: 10.1002/joc

(b) Month	Distance (km)									
	0–50		50–150		150–350		350–700		700–1400	
	Mean	Standard deviation	Mean	Standard deviation	Mean	Standard deviation	Mean	Standard deviation	Mean	Standard deviation
January	0.735	0.203	0.646	0.261	0.470	0.329	0.294	0.362	0.218	0.313
February	0.823	0.165	0.765	0.184	0.668	0.215	0.576	0.232	0.374	0.308
March	0.802	0.187	0.734	0.204	0.609	0.244	0.482	0.273	0.271	0.332
April	0.660	0.311	0.589	0.294	0.421	0.329	0.225	0.346	0.083	0.326
May	0.635	0.289	0.588	0.276	0.494	0.308	0.392	0.321	0.379	0.297
June	0.640	0.252	0.532	0.276	0.428	0.294	0.301	0.313	0.124	0.338
July	0.515	0.303	0.425	0.315	0.304	0.349	0.123	0.359	−0.091	0.341
August	0.447	0.320	0.338	0.330	0.256	0.336	0.176	0.348	0.124	0.347
September	0.648	0.299	0.547	0.319	0.372	0.357	0.188	0.382	−0.027	0.351
October	0.751	0.192	0.679	0.228	0.549	0.288	0.350	0.349	0.321	0.363
November	0.755	0.205	0.662	0.273	0.525	0.325	0.338	0.377	−0.010	0.327
December	0.723	0.279	0.632	0.327	0.437	0.400	0.407	0.378	0.134	0.416

Table IV. Monthly correlation's statistics of (a) daily rainfall events and (b) monthly number of rainy days, according to distance-based classes.

(a) Month	Distance (km)									
	0–50		50–150		150–350		350–700		700–1400	
	Mean	Standard deviation	Mean	Standard deviation	Mean	Standard deviation	Mean	Standard deviation	Mean	Standard deviation
January	0.597	0.184	0.524	0.193	0.442	0.195	0.315	0.183	0.122	0.131
February	0.617	0.168	0.519	0.198	0.446	0.193	0.309	0.183	0.073	0.126
March	0.623	0.159	0.539	0.188	0.449	0.183	0.307	0.173	0.116	0.126
April	0.615	0.162	0.519	0.170	0.432	0.166	0.289	0.162	0.085	0.117
May	0.533	0.201	0.426	0.190	0.326	0.173	0.201	0.156	0.043	0.115
June	0.467	0.158	0.368	0.165	0.273	0.149	0.157	0.129	0.010	0.109
July	0.402	0.150	0.290	0.151	0.204	0.134	0.100	0.117	−0.005	0.101
August	0.418	0.161	0.322	0.161	0.239	0.148	0.122	0.123	−0.012	0.104
September	0.549	0.187	0.436	0.188	0.347	0.164	0.192	0.151	0.001	0.102
October	0.598	0.158	0.497	0.166	0.411	0.167	0.265	0.168	0.048	0.118
November	0.633	0.140	0.545	0.175	0.458	0.180	0.290	0.179	0.063	0.120
December	0.593	0.177	0.513	0.198	0.447	0.192	0.311	0.186	0.106	0.122

(b) Month	Distance (km)									
	0–50		50–150		150–350		350–700		700–1400	
	Mean	Standard deviation	Mean	Standard deviation	Mean	Standard deviation	Mean	Standard deviation	Mean	Standard deviation
January	0.555	0.307	0.539	0.298	0.485	0.303	0.379	0.322	0.287	0.309
February	0.673	0.241	0.676	0.213	0.621	0.244	0.485	0.297	0.159	0.342
March	0.636	0.254	0.573	0.310	0.469	0.368	0.408	0.376	0.195	0.368
April	0.623	0.270	0.578	0.273	0.476	0.305	0.280	0.349	0.020	0.349
May	0.637	0.293	0.607	0.295	0.544	0.312	0.449	0.318	0.265	0.321
June	0.663	0.273	0.647	0.241	0.563	0.265	0.414	0.309	0.171	0.374
July	0.553	0.247	0.503	0.273	0.405	0.306	0.246	0.330	−0.072	0.343
August	0.499	0.296	0.479	0.272	0.413	0.288	0.287	0.310	0.125	0.341
September	0.608	0.285	0.542	0.280	0.402	0.312	0.197	0.337	0.014	0.357
October	0.738	0.181	0.691	0.243	0.637	0.257	0.459	0.347	0.145	0.314
November	0.631	0.281	0.584	0.306	0.539	0.310	0.356	0.376	0.166	0.369
December	0.566	0.316	0.498	0.319	0.416	0.333	0.253	0.366	0.017	0.385

DOI: 10.1002/joc

period, rainfall amounts in Alabama, Florida and Georgia were found to have a geographical trend described by a first degree polynomial during December to April and a third degree polynomial during the remaining months.

Using both daily and monthly rainfall data, two well-defined rainfall spatial correlation patterns were found corresponding to the frontal and the convective rainy seasons. Spatial correlations during the frontal rainy season were characterized by a widely spread pattern in a northeast–southwest direction around weather stations, which is perpendicular to the usual weather front paths. During the convective rainy season, correlations were characterized by small concentric patterns in which correlations decreased rapidly over short distances from each weather station. However, larger areas of higher correlations were found using monthly rainfall amounts than when using daily rainfall amounts. Spatial correlations among daily rainfall amounts and occurrence of events are needed for spatial weather generators on a storm-by-storm basis. Spatial correlations among monthly rainfall amounts and rainfall persistence are needed to ensure the validity of downscaled data from numerical seasonal rainfall forecasts.

ACKNOWLEDGEMENTS

The research was supported by the National Oceanic and Atmospheric Administration – Applied Research Center (NOAA-ARC) through the Grant No. NA16GP1365 subcontract FSU/UF No. 02081352-1-1 and developed under the auspices of the Southeast Climate Consortium. The views expressed in this paper are those of the authors and do not necessarily reflect the views of NOAA or any of its subagencies.

REFERENCES

Baigorria GA, Romero CC. 2006. Assessment of erosion hotspots in a watershed: integrating the WEPP model and GIS in a case study in the Peruvian Andes. *Environmental Modelling & Software* Doi: 10.1016/j.envsoft.2006.06.012. In press, Corrected Proof, available online 22 August 2006.

Baigorria GA. 2005. Climate interpolation for land resource and land use studies in mountainous regions. Dissertation thesis, Wageningen University and Research Centre, Wageningen, The Netherlands, 168 p.

Bonan GB, Oleson KW, Vertenstein M, Levis S, Zeng X, Dai Y, Dickinson RE, Yang ZL. 2002. The land surface climatology of the community land model coupled to the NCAR community climate model. *Journal of Climate* **15**: 3123–3149.

Briggs WM, Wilks D. 1996. Extension of the CPC long-lead temperature and precipitation outlooks to general weather statistics. *Journal of Climate* **9**: 3496–3504.

Clark I, Harper WV. 2001. *Practical Geostatistics 2000*. Ecosse North America Llc, publishers: Westerville, OH; 342.

Clark MP, Gangopadhyay S, Brandon D, Werner K, Hay L, Rajagopalan B, Yates D. 2004. A resampling procedure for generating conditioned daily weather sequences. *Water Resources Research* **40**: 1–15.

Cocke S, LaRow TE. 2000. Seasonal predictions using a regional spectral model embedded within a coupled ocean-atmosphere model. *Monthly Weather Review* **128**: 689–708.

Davis RE, Hyden BP, Gay DA, Phillips WL, Jones GV. 1997. The North Atlantic Subtropical Anticyclone. *Journal of Climate* **10**: 728–744.

Fowler HJ, Kilsby CG, O'Connell PE, Burton A. 2005. A weather-type conditioned multi-site stochastic rainfall model for the generation of scenarios of climatic variability and change. *Journal of Hydrology* **308**: 50–66.

Fraisse CW, Baigorria GA, Pathak TB. 2006. Spatial analysis of freeze events in Florida. *Proc Fla State Hort Soc* **119**: In press.

Goovaerts P. 1997. *Geostatistics for Natural Resources Evaluation*. Oxford University Press: Oxford; 483.

Grondona MO, Podestá GP, Bidegain M, Marino M, Hordij H. 2000. A stochastic precipitation generator conditioned on ENSO phase: a case study in southeastern South America. *Journal of Climate* **13**: 2973–2986.

Hansen JW, Indeje M. 2004. Linking dynamic seasonal climate forecasts with crop simulation for maize yield prediction in semi-arid Kenya. *Agricultural and Forest Meteorology* **125**: 143–157.

Huang J, van den Dool HM, Barnston AG. 1996. Long-lead seasonal temperature prediction using optimal climate normals. *Journal of Climate* **9**: 809–817.

Isaaks EH, Srivastava RM. 1989. *An Introduction to Applied Geostatistics*. Oxford University Press: New York; 561.

Jian X, Olea RA, Yu YS. 1996. Semivariogram modeling by weighted least squares. *Computers & Geosciences* **22**: 387–397.

Jones JW, Hoogenboom G, Porter CH, Boote KJ, Batchelor WD, Hunt LA, Wilkens PW, Singh U, Gijsman AJ, Ritchie JT. 2003. The DSSAT cropping system model. *European Journal of Agronomy* **18**: 235–265.

Karl TR, Jones PD, Knight RW. 1993. Asymmetric trends of daily maximum and minimum temperatures. *Bulletin of the American Meteorological Society* **74**: 1007–1023.

Konrad CE. 1994. Moisture trajectories associated with heavy rainfall in the Appalachian region on the United States. *Physical Geography* **15**: 227–248.

Maul GA, Hanson K. 1990. A century of southeastern United States climate change observations: temperature, precipitation, and sea level. In *Global Change: A Southern Perspective*, Proceedings 1990 Southeast Climate Symposium. Southeast Regional Climate Center: Columbia, SC; 139–155.

Parlange MB, Katz RW. 2000. An extended version of the Richardson model for simulating daily weather variables. *Journal of Applied Meteorology* **39**: 610–622.

Podestá G, Letson D, Messina C, Royce F, Ferreira RA, Jones JW, Hansen JW, Llovet I, Grondona M, O'Brien JJ. 2002. Use of ENSO-related climate information in agricultural decision making in Argentina: a pilot experience. *Agricultural Systems* **74**: 371–392.

Racsko P, Szeidl L, Semenov M. 1991. A serial approach to local stochastic weather models. *Ecological Modelling* **57**: 27–41.

Richardson CW, Wright DA. 1984. *WGEN: A Model for Generating Daily Weather Variables*. U.S. Department of Agriculture, Agricultural Research Service: Washington, DC, ARS-8; 83.

Robinson PJ, Henderson KG. 1992. Precipitation events in the Southeast United States of America. *International Journal of Climatology* **12**: 701–720.

Romero CC, Baigorria GA. 2006. Changes of erosive rainfall for El Niño and La Niña years in the northern Andean Highlands of Peru: The case of La Encañada watershed. *Climatic Change* In press.

Schoof JT, Arguez A, Brolley J, O'Brien JJ. 2005. A new weather generator based on spectral properties of surface air temperatures. *Agricultural and Forest Meteorology* **135**: 241–251.

Sharon D. 1974. On the modelling of correlation functions for rainfall studies. *Journal of Hydrology* **22**: 219–224.

Shin DW, Cocke S, LaRow TE, O'Brien JJ. 2005. Seasonal surface air temperature and precipitation in the FSU Climate Model coupled to the CLM2. *Journal of Climate* **18**: 3217–3228.

Soule PT. 1993. Hydrologic drought in the contiguous United States, 1900–1989: spatial patterns and multiple comparisons of means. *Geophysical Research Letters* **20**: 2367–2370.

Southeast Regional Assessment Team. 2002. Preparing for a changing climate: the potential consequences of climate variability and change – Southeast, U.S. Global Change Program.

Stahle DW, Cleaveland MK. 1992. Reconstruction and analysis of spring rainfall over the Southeastern U.S. for the past 1000 years. *Bulletin of the American Meteorological Society* **73**: 1947–1961.

Sumner GN. 1983. The use of correlation linkages in the assessment of daily rainfall patterns. *Journal of Hydrology* **66**: 169–182.

USGS. 2006. Status and Trends of the Nation's Biological Resources. [Online] Available at: http://biology.usgs.gov/s+t/SNT/index.htm. Verified: March 20th 2006.

Vedwan N, Broad K, Letson D, Ingram KT, Podestá G, Breuer NE, Jones JW, O'Brien JJ. 2005. Assessment of climate information dissemination efforts by the Florida Climate Consortium. The

Southeast Climate Consortium Technical Report Series. Technical Report SECC-05-001. Gainesville, FL.

Walsh JE, Richman MB, Allen DW. 1982. Spatial coherence of monthly precipitation in the United States. *Monthly Weather Review* **110**: 272–286.

Webster R, McBratney AB. 1989. On the Akaike Information criterion for choosing models for variograms of soil properties. *Journal of Soil Science* **40**: 493–496.

Whelan BM, McBratney AB, Minasny B. 2001. Spatial prediction software for precision agriculture. In *ECPA 2001. Proceedings of the 3rd European Conference of Precision Agriculture*, Grenier G, Blackmore S (eds) Agro Montpellier, Ecole Nationale Agronomique de Montpellier: Montpellier; 139–144.

Wilks DS. 2002. Realizations of daily weather in forecast seasonal climate. *Journal of Hydrometeorology* **3**: 195–207.

Zeng X, Shaikh M, Dai Y, Dickinson RE, Myneni R. 2002. Coupling of the common land model to the NCAR community climate model. *Journal of Climate* **15**: 1832–1854.

DOI: 10.1002/joc